Romanian Reports in Physics **69**, 610 (2017)

A FINITE ELEMENT METHOD MODEL TO SIMULATE THE THERMAL RESPONSE OF VASCULARIZED TISSUE TO LASER IRRADIATION

P. BARVINSCHI, O.M. BUNOIU*

West University of Timisoara, Faculty of Physics, 4 V. Parvan Avenue, 300223 Timisoara, Romania,
*Corresponding author: madalin.bunoiu@e-uvt.ro

Received May 20, 2016

Abstract. In this study we developed a numerical model for calculating the heating effects of a laser beam on biological tissues, taking into considerations the cooling effects of flow in the blood vessels traversing the tissue. Because the laser radiation is supposed to be provided by a CO_2 laser the volumetric heat source has a very small thickness at the surface of the tissue and it can be calculated using the Beer-Lambert's law. At the vessel entrance the blood flow is supposed to have a parabolic profile. The transient heat equation with a convection term was solved using the finite element method. A parametric study was conducted in order to see the effects of the blood flow network and laser parameters on the temperature field in the vascularized tissue. The results of the calculations suggest that the temperature distribution into the vascularized tissue depends on the laser power, laser spot size, blood vessels size and position, and blood flow rate.

Key words: computer simulation, photo-thermal heating, vascularized tissue.

1. INTRODUCTION

Lasers have been widely used in therapeutic applications for more than three decades [1–9]. The majority of laser applications in medicine do involve thermal effects. The extent of thermal destruction of tissue by laser radiation is governed by i) heat deposition in the tissue, ii) heat transfer, and iii) temperature-dependent rate reactions. The deposition of energy into the tissue is not only a function of laser irradiation parameters (power, exposure time, laser spot diameter), but it also depends upon the absorption and scattering properties of the tissue. Moreover, the depth of laser penetration in the irradiated tissue depends on the laser wavelength. Once the rate of energy deposition is established, it is possible to calculate the temperature field in the irradiated tissue by using the heat transfer theory and assuming suitable boundary conditions. Increasing the tissue temperature may cause hyperthermia, coagulation, vaporization, carbonization or melting of the

living tissue. By laser hyperthermia we understand the therapeutic procedure where the laser beam heats a localized tumor volume beyond its normal value (ranging approximately 42–60 ^{o}C for humans) with the hope that the heat treatment may cause remission (destruction of specific cells/tissues).

Even homogeneous tissues are turbid media and both absorption and scattering of radiation are present simultaneously in a tissue [5–6]. Chemists and physicists use Beer-Lambert's law when they calculate the loss of energy in the incident beam by absorption of light. On the other hand, scattering of a photon is accompanied by a change in the propagation direction without loss of energy. According to the size of the scattering structure of the tissue one can distinguish between Rayleigh scattering (large structures, like membranes, collagen fibers, macromolecules) and Mie scattering (small structures, like mitochondria, lysosomes, vesicles). Mie scattering can be calculated using Monte Carlo simulations. If scattering is predominantly in a forward direction the photon density into tissue can be described by the diffusion approximation of the transport theory. The choice of the appropriate model used to calculate the photon distribution into tissues depends on the values for μ_a (absorption coefficient) and $\mu_s^{'} = \mu_s(1-g)$ (reduced scattering coefficient, where μ_s = scattering coefficient and g = anisotropy factor) [10]: i) $\mu_a >> \mu_s^{'}$: the Beer-Lambert's law is valid ($\lambda <$ 300 nm and $\lambda >$ 2,000 nm); ii) $\mu_a << \mu_s^{'}$: the diffusion approximation is valid (650 nm $< \lambda <$ 1,150 nm); iii) $\mu_a \approx \mu_s^{'}$: the transport equation with Monte Carlo simulation is valid (300 nm $< \lambda <$ 650 nm and 1,150 nm $< \lambda <$ 2,000 nm). In the case of living tissues with a complex morphology, like vascularized tissues or tumors buried in normal tissues, the calculation of the photon distribution can be performed by using the diffusion approximation or Monte Carlo simulations. The Beer-Lambert's law can be used in such cases only when the tissue can be considered as being homogeneous in the region exposed to the incident beam and having a thickness comparable with the penetration depth of the radiation. Although some authors [11–12] used a heuristic version of the Beer-Lambert's law proposed by Motamedi *et al*. [13], that modify the magnitude and shape of the light distribution by taking into consideration both absorption and scattering of photons, it is important to note that this version of Beer-Lambert's law can be used only in homogeneous turbid media and not in a tissue having a complex morphology, like a vascularized one.

In this work we present a study concerning the distribution of heat in tissues embedded with blood vessels during laser-assisted photo-thermal hyperthermia. The problem of the convective effects of blood flow in vessels on the temperature distribution in the treated tissue is not a new one. We can mention here the early works of Chato [14], Lagendijk [15], Charny and Levin [16], Chen and Roemer [17], Kolios *et al*. [18]. More recently, Zhou and Liu [19] and Shih *et al*. [20] proposed 3-D theoretical models of light and heat transport in a laser irradiated tissue with different sizes embedded blood vessels. Mohammed and Verkey [21]

developed a 3-D model for the use of LITT (Laser Interstitial Thermo Therapy) in sensitive area such as the neck region to treats tumors in lymph node near the carotid artery.

In the study proposed by Paul *et al*. [12] the thermal effects of large blood vessels on temperature evolution in tissue subjected to laser irradiation is calculated using the finite element method. A volumetric source term based on the heuristic Beer-Lambert's law proposed in [13] is introduced into the energy equation to account for laser heating. In fact, the laser heat generation in the homogeneous tissue, in the blood vessel, and in the liquid blood was calculated using the same analytical form of Beer-Lambert's law, taking different physical and optical properties for each of the three media. The optical properties of the tissue, vessel wall and blood used in the mentioned work correspond to a laser wavelength of 1064 nm (NIR region, Nd:YAG laser); at this wavelength the tissue transmission is highest.

In our opinion, they are two questionable points in the study of Paul *et al*. [12]. Firstly, for the mentioned laser wavelength (1064 nm) the photon distribution into the vascularized tissue must be calculated using the diffusion approximation of the transport theory and not the Beer-Lambert law [10]. Secondly, even if Beer-Lambert's law should be applied, it is not appropriate to calculate the heat generation using the same analytical form of this law in the three media (tissue, vessel wall, and blood) because the laser power and beam size appearing in this law are well established parameters at only the tissue-air interface and not at the tissue-vessel wall and respectively vessel wall-blood interfaces.

These two observations motivated the present study. We developed a suite of 3-D models for tissues embedded with blood vessels and subjected to laser irradiation. In order to avoid the questionable points in the work of Paul *et al.* [12] we selected the 10600 nm CO_2 laser radiation. The value of the absorption coefficient in living tissues at this wavelength is very large (about 800 cm^{-1}) and the penetration depth is very small (about 10–17 μm). The volumetric heat source is then limited to a very thin region at the tissue surface and the radiation does not reach the buried blood vessels, tumors, or other inhomogeneous regions in the tissue. We considered laminar flow of the blood with a parabolic velocity profile in the vessel. The transient heat equation with a convection term was solved using the finite element method. A parametric study was made in order to see the effects of the blood flow and laser parameters on the temperature field in the vascularized tissue.

2. MODEL DESCRIPTION AND IMPLEMENTATION

2.1. MODEL GEOMETRY AND PHYSICAL PROPERTIES

In order to evaluate the cooling effect of blood flow in vessels on tissue temperature during laser irradiation a suite of 3D vascularized tissue models was

developed. The geometry of these models is based on a block of tissue having the dimensions 40 mm × 40 mm × 10 mm in x, y, and z-direction respectively.

Table 1

Thermo-physical properties of skin layers, blood, and blood flow parameters used in simulations

Tissue layers	Thickness [mm]	ρ [kg m^{-3}]	K [W m^{-1} K^{-1}]	C [J kg^{-1} K^{-1}]	Q_{met} [W m^{-3}]
Epidermis	0.2	1200	0.235	3589	0
Dermis	1.8	1200	0.445	3300	368.1
Hypodermis	2	1000	0.185	2674	368.3
Muscle	6	1085	0.51	3800	684.2
Blood vessel in:	Radius [mm]	ρ [kg m^{-3}]	K [W m^{-1} K^{-1}]	C [J kg^{-1} K^{-1}]	u_{max} [cm s^{-1}]
Dermis	0.13 0.18	1060	0.501	3770	1.8 2.5
Hypodermis	0.4				5.0
Muscle	0.5				7.0

For the validation of our model we have used a single homogeneous layer of tissue, but in our parametric study on more complex models we have used a multilayered tissue having the structure of the human skin. In the case of vascularized tissue models we have considered one or more blood vessels buried at different depths into the tissue and transiting it in the x-direction. Other details will be given in the forthcoming sections.

For the thermo-physical properties of skin layers and blood, as well as blood flow parameters, we have taken the values reported in [22]; the data are tabulated in Table 1.

2.2. MATHEMATICAL MODEL

2.2.1. Governing equations

The numerical study has been carried out by dividing the computational domain into two subdomains: i) tissue (skin) subdomain, and ii) the vascular (blood vessels) subdomain. In order to determine the temperature distribution in the perfused tissue the Pennes bioheat equation [23] was used by many authors. The bioheat equation is the expression of the principle of conservation of energy applied to a tissue volume and it is written as

$$\rho C \frac{\partial T}{\partial t} = \nabla \cdot (k \nabla T) + \rho_b C_b \omega_b (T_b - T) + Q_{met} + Q_{ext}\,, \tag{1}$$

where ρ, C, and k are the density, specific heat and thermal conductivity of the tissue, ρ_b and C_b are the density and specific heat of the blood, ω_b is the blood perfusion rate within the tissue, T_b is the temperature of arterial blood, T is the local tissue temperature, Q_{met} is the volumetric heat generation due to metabolism, and Q_{ext} is a volumetric external heat source. The contribution of the metabolic heat source is extremely small in our simulations and therefore we have taken $Q_{met} = 0$. In our simulations the external heat results from the interaction of laser radiation with the tissue. As stated in the introduction, the laser radiation considered in the present study is that provided by a CO_2 laser. Because CO_2 laser radiation is highly absorbed in tissue its penetration depth has a very small value compared to the thickness of epidermis. On the other hand, the scattering of CO_2 radiation is much smaller than the absorption in tissue and we have taken it as being zero. In these conditions the volumetric external heat source can be written [5]

$$Q_{ext} = \mu_a I(r,z)\, F(t)\,, \tag{2}$$

where μ_a [cm^{-1}] is the absorption coefficient of the radiation in the epidermis, $I(r, z)$ [Wm^{-2}] is the intensity (light fluence rate) of the radiation at depth z in the epidermis and at distance $r = \sqrt{x^2 + y^2}$ from the axis of the laser beam. The function $F(t)$ in eq. (2) gives the temporal distribution of the laser pulse train (laser exposure function). It will be shown that this heat source is completely embedded in epidermis. Taking into consideration that the radial laser beam dimensions are typically 500 μm or larger, which is much larger than the CO_2 laser radiation penetration depth in tissue, this situation can be modeled by assuming that the tissue is a semi-infinite medium in air. For a Gaussian-shaped laser beam the irradiance $I(r)$ [Wm^{-2}] can be written [5]

$$I(r) = \frac{P_0}{\left(\pi r_0^2 / 2\right)} \exp\left(-\frac{2r^2}{r_0^2}\right) = I_0 \exp\left(-\frac{2r^2}{r_0^2}\right), \tag{3}$$

where P_0 is the total laser power, $I_0 = P_0 / \left(\pi r_0^2 / 2\right)$ is the maximum irradiance, and r_0 is the $1/e^2$-radius of the laser beam. For the irradiance considered in equation (3) and assuming an exponential axial attenuation with absorption coefficient μ_a the fluence rate $I(r, z)$ is given by the Beer-Lambert's law and we have [5]

$$I(r,z) = I_0 \exp\left(-\frac{2r^2}{r_0^2}\right) \exp\left(-\mu_a z\right); \tag{4}$$

this expression must be used in the external heat source Q_{ext} given by equation (2).

The heat convection between tissue and a large vessel can be thought as occurring as a direct energy transfer rather than perfusion. Therefore, the perfusion term in the bioheat equation (1) may be modified to consider internal energy flow out of the control tissue volume by means of the blood flow (convection). The resulting equation for the energy transport by the blood flow in the vessels can by modeled by considering diffusion and convection heat transfer as follows:

$$\rho_b C_b \frac{\partial T}{\partial t} = \nabla \cdot (k_b \nabla T) - \rho_b C_b (\vec{u} \cdot \nabla T), \tag{5}$$

where $\vec{u}$ is the blood velocity. The energy transport in the skin layers was modeled using a diffusion heat transfer in each layer, as follows:

$$\begin{aligned} \rho_e C_e \frac{\partial T}{\partial t} &= \nabla \cdot (k_e \nabla T) + Q_{ext}, \\ \rho_d C_d \frac{\partial T}{\partial t} &= \nabla \cdot (k_d \nabla T), \\ \rho_f C_f \frac{\partial T}{\partial t} &= \nabla \cdot (k_f \nabla T), \\ \rho_m C_m \frac{\partial T}{\partial t} &= \nabla \cdot (k_m \nabla T), \end{aligned} \tag{6}$$

where the subscripts *e*, *d*, *f*, and *m* refers to epidermis, dermis, fat and muscle respectively. Q_{ext} in the first equation (6) is the volumetric laser heat source given by (2); due to the small penetration depth of the CO_2 laser radiation Q_{ext} acts only in the epidermis.

2.2.2. Boundary conditions

The tissue top surface was subjected to natural convection cooling and the convective heat loss coefficient to ambient air (T_{air} = 23°C) was taken as h = = 10 W m^{-2} K^{-1} [25]. It is known that skin behaves as a black surface and has an emissivity close unity (ε = 0.98) [22]; due to the small temperature difference between skin and air we neglected the surface radiation. On the other surfaces of the skin sample a *thermally insulated* boundary condition was considered. At the artery entrance the parabolic velocity profile $u(y,z)$ in the positive x-direction can be written [25]

$$u(y,z) = u_{\max}\left[1 - \frac{(y-y_c)^2 + (z-z_c)^2}{R^2}\right], \tag{7}$$

where $u_{\max}$ is the value of the velocity in the middle of the vessel, y_c and z_c are the coordinates of the vessel entrance center, and R is the vessel radius. The same

velocity profile was considered at the vein entrance but in the opposite direction. For the blood flow *no slip* boundary condition was imposed on the vessel wall. The temperature of the blood at the inlet of the blood vessel was considered to be 37 ^{o}C. At the vessels outlets convection dominates the transport of heat so we applied the convective flux boundary condition, $-k\nabla T \cdot \vec{n} = 0$, where $\vec{n}$ is the normal to the outlet surface.

2.3. COMPUTING DETAILS

The governing equations of the models were solved using the finite element method as provided by the commercial software COMSOL Multiphysics 3.5 [26] in the application mode Transient General Heat Transfer. A tetrahedral meshing scheme with about 6,800,000 elements was generated for each model. The model equations were solved transiently using the generalized minimum residual (GMRES) iterative method and the backward differentiation formula (BDF) was used for time stepping; the time step was 0.1 s. For the stabilization of the convective heat transfer we have used the Galerkin least square (GLS) method. The convergence was reached in less than 50 iterations. The computing time was about 30 minutes for 100 seconds of real time simulation. All the calculations were done on a simple PC with an Intel Core i7-4790K CPU and 4 GHz, with 16 GB RAM.

3. RESULTS AND DISCUSSIONS

3.1. MODEL VALIDATION

In order to check the correctness of the mathematical model described in the previous sections the calculated results were evaluated in comparison to the temperature measurements in a soft biological material reported in [27]. The case 2 in the results section of the reference [27] reports on experiments performed to measure the temperature field in egg albumin (egg white) at room temperature exposed to a CO_2 laser pulse (laser power P_0 = 5W, pulse length t_p = 0.1 s, radius of the Gaussian beam r_0 = 3.4 mm). The thermal parameters for egg albumin considered in numerical calculations were $k = 5.56 \cdot 10^{-3}$ W cm^{-1}K^{-1}, ρ = = 1.036 g cm^{-3}, and C = 3.36 J g^{-1} K^{-1}. The value for the absorption coefficient was set to μ_a = 767 cm^{-1}. The geometry for computing the temperature in the egg albumin was a cylindrical one, with radius R = 0.5 cm and height z = 1 cm. Figure 1 shows the temperature rise calculated with our model at two different

locations inside the egg albumin, points P_1 ($r = 0$; $z = 9.8$ mm) and P_2 ($r = 0.8$ mm; $z = 9.2$ mm); these points are the same as those used in the experimental measurements reported in [27]. We have used the following boundary conditions: zero temperature gradient normal to the symmetry axis; thermal insulation on the other boundaries. The agreement between our results and those presented in Fig. 5 of reference [27] is very good.

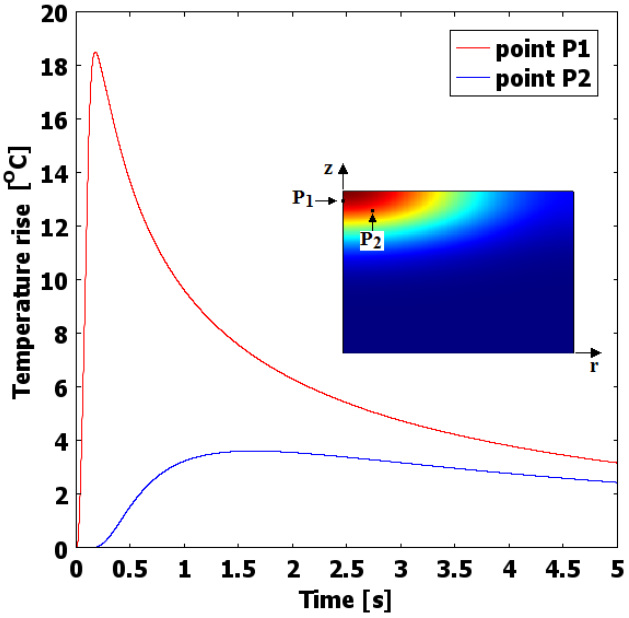

Fig. 1 – Calculated temperature rises at two points in egg-albumin under CO_2 laser irradiation.

3.2. PARAMETRIC STUDY IN A SINGLE VESSEL TISSUE

In a numerical simulation of the thermal response of a laser irradiated vascularized tissue the main parameters which affect the temperature distribution are the thermo-physical parameters of the tissue, the position of the blood vessel relative to the tissue surface, the blood flow rate, and the laser irradiation parameters (power, spot size, exposure time). The models described in this section are developed taking into consideration a homogeneous tissue with dimensions 40 mm × 40 mm × 10 mm in x, y, and z-direction respectively and a single blood vessel transiting the tissue in the x-direction. As homogeneous tissue we have

considered the dermis layer of the human skin, whose thermo-physical parameters are given in Table 1. The radius of the blood vessel was fixed to R = 0.4 mm. The value for the absorption coefficient was taken as μ_a = 767 cm^{-1}. The initial tissue temperature and the blood temperature at the inlet of the vessel were set to 37°C. The boundary conditions were those described in section 2.2.2. The exposure time for laser irradiation was 100 s in each case.

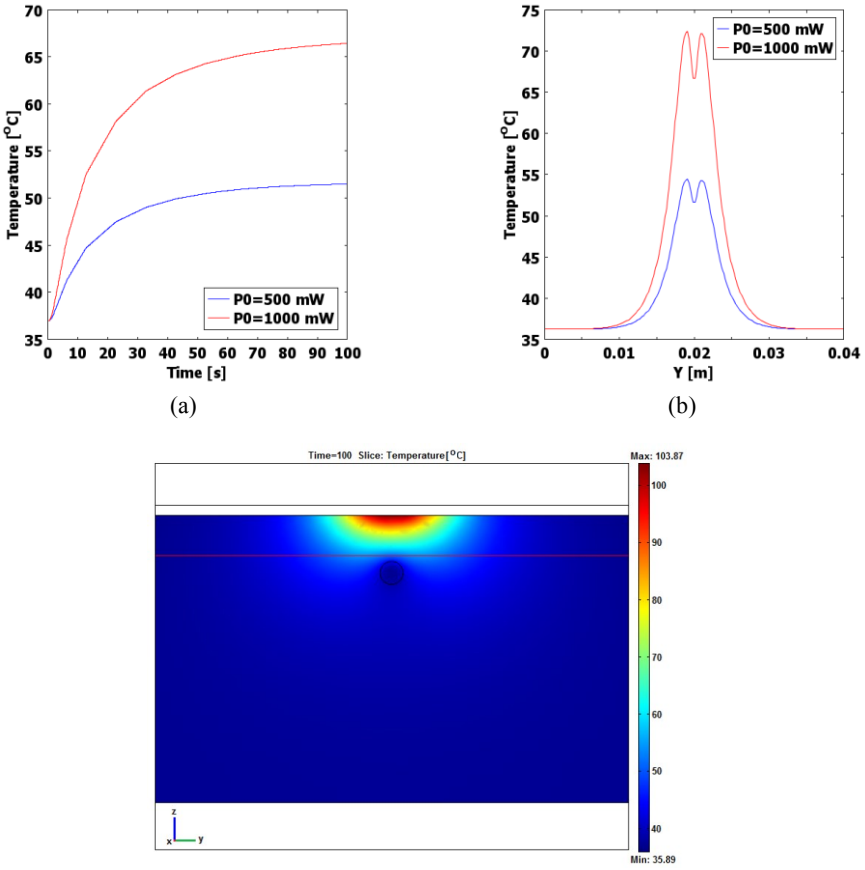

Fig. 2 – Effect of laser power on the temperature distribution in the tissue containing a single blood vessel: temperature *vs.* time (a) and temperature *vs.* *y*-coordinate (b). The *y*-coordinate in (b) is along the red line shown in (c).

3.2.1. Effect of laser power

A single blood vessel having a radius R = 0.4 mm and a flow rate in the x direction with maximum velocity u_{max} = 5 cm s^{-1} was considered in this model;

the center of the vessel was at a depth of 2 mm from the top tissue surface and it transits the entire tissue. The laser beam was supposed to have a Gaussian profile with r_0 = 2.5 mm. The temperature distribution in the tissue was calculated for two values of the total laser power (P_0), 500 mW and 1000 mW respectively. We have evaluated the differences between the two cases by calculating the temperature *vs.* time at the point having the coordinates (0.02; 0.02; 0.0084) and the temperature *vs. y*-coordinate along the line normal to the blood vessel and having its ends at points (0.02; 0; 0.0086) and (0.02; 0.04; 0.0086) (all the coordinates are given in meters). The results of these calculations are shown in Fig. 2 and we see that as the laser power increases, the tissue temperature also increases. Figure 2a shows that the irradiation time of 100 s was large enough for approaching a (maximum) steady temperature. The camel hump shape of the $T(y)$ profile in Fig. 2b is due to the cooling effect of the blood flow, as is clearly observed in Fig. 2c.

3.2.2. Effect of laser spot size

The laser spot size r_0 is an important parameter in laser-assisted photo-thermal therapy. In order to demonstrate its influence on the temperature distribution in the irradiated vascularized tissue we have used the same model as in the previous section, where we set the laser power as P_0 = 500 mW. The calculations were performed for two values of r_0, 2.5 mm and 5 mm respectively. Figures 3a–b show the dependencies $T(t)$ and $T(y)$ for the two values of laser beam radius. As expected, there is an increasing in the tissue temperature with the decreasing of laser spot size because for the same power the intensity increases with decrease of the laser spot size.

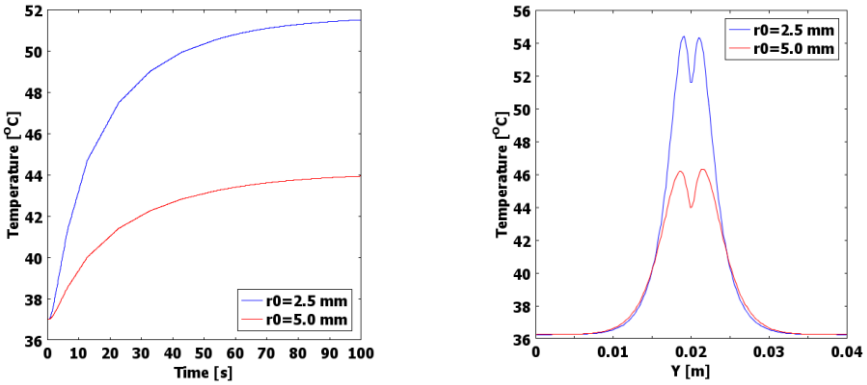

(a) (b)

Fig. 3 – Effect of laser spot size on the temperature distribution in the tissue containing a single blood vessel: temperature *vs.* time (a) and temperature *vs. y*-coordinate (b).

3.2.3. Effect of the blood vessel depth

In order to demonstrate the influence of the blood vessel position on the temperature distribution in the irradiated tissue we considered a single vessel with radius R = 0.4 mm and maximum flow rate velocity u_{max} = 5 cm s^{-1}, the center of the vessel being situated at 2 mm and 3 mm respectively from the top tissue surface. The power of the laser beam was set as P_0 = 500 mW and the radius of the beam was taken to be r_0 = 2.5 mm. The results of the calculations are shown in Fig. 4 and we see that the cooling effect of the blood flow reduces with the increase of the depth of the vessel. Obviously, the cooling effect is more important near the blood vessel than in the points situated at larger distances from the vessel.

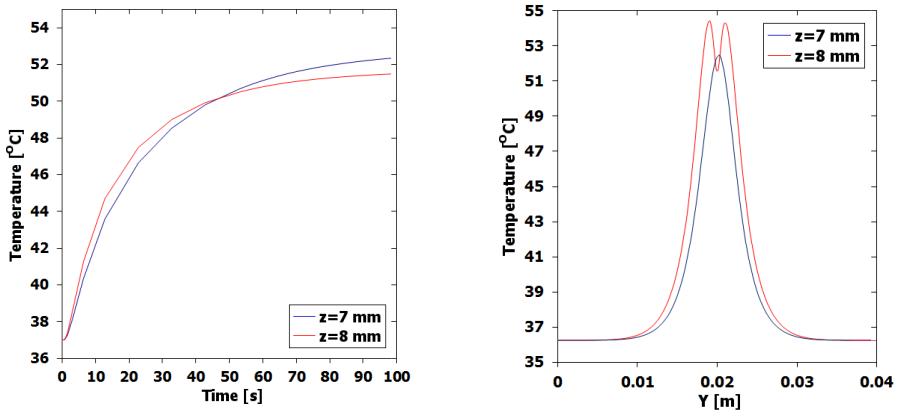

(a) (b)

Fig. 4 – Effect of blood vessel depth on the temperature distribution in the tissue containing a single blood vessel: temperature *vs.* time (a) and temperature *vs.* *y*-coordinate (b).

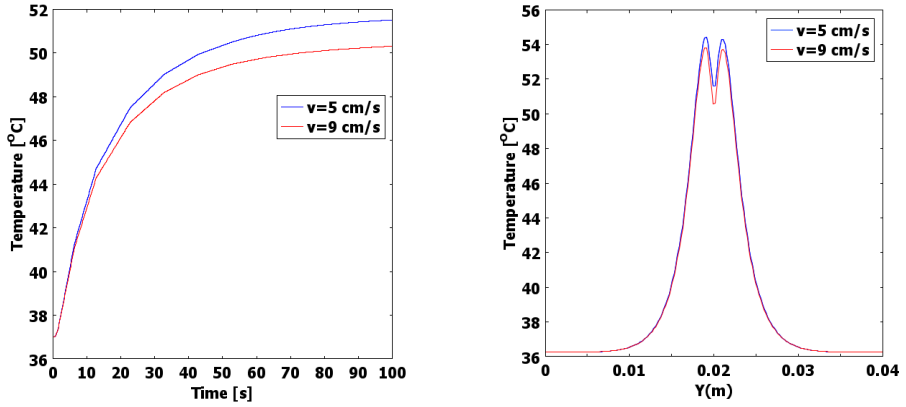

(a) (b)

Fig. 5 – Effect of blood flow rate on the temperature distribution in the tissue containing a single blood vessel: temperature *vs.* time (a) and temperature *vs.* *y*-coordinate (b).

3.2.4. Effect of blood flow rate

In this case we have considered a vessel with radius R = 0.4 mm whose center is situated at 2 mm from the top tissue surface. For the maximum flow rate velocity u_{max} we have taken the values 5 cm s^{-1} and 9 cm s^{-1} respectively. As expected, the behavior of the thermal field in the system under study is sensitive to the convective heat transfer parameters and the cooling effect of the single blood vessel increases with increase of the flow rate velocity (Fig. 5).

3.3. COOLING EFFECT IN A VASCULARIZED SKIN

In order to better demonstrate the cooling effect of blood flow on tissue temperature during laser irradiation a suite of vascularized skin models was considered. Human skin consists of four layers: epidermis, dermis, fat, and muscle. Excepting the epidermis, each layer of the skin contains a vessel network and the flow of blood takes place in a counter-current artery-vein pair arrangement. The skin block in our models has the dimensions 40 mm × 40 mm × 10 mm in x, y, and z-direction respectively. The geometry of the skin layers and the blood vessels positions within the skin, considered in this work, are indicated in Fig. 6. The velocity within the artery is in the positive x-direction and the velocity within the vein is in the negative x-direction. For the thermo-physical properties of the skin layers and the blood flow parameters we have taken the values tabulated in Table 1.

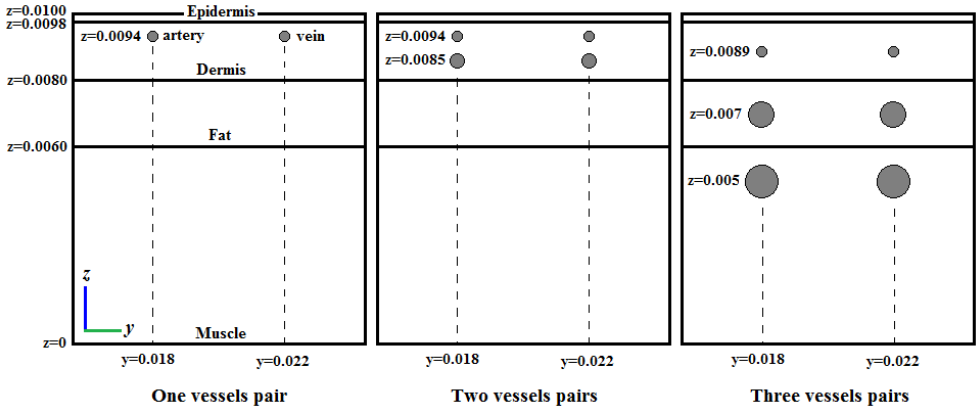

Fig. 6 – Geometry of the skin layers and the blood vessels positions within the skin.

The initial tissue temperature and the blood temperature at the inlet of the blood vessel were set to 37°C. The boundary conditions were those described in section 2.2.2. Because the penetration depth of CO_2 laser beam is smaller than the

epidermis thickness we have considered a single value for the absorption coefficient, μ_a = 767 cm^{-1}. The exposure parameters were as follows: laser peak power P_0 = 500 mW, radius of the Gaussian beam r_0 = 2.5 mm, and a temporal distribution of the pulse train $F(t)$ having a rectangular profile with a pulse length t_p = 1 s.

The results of the calculations are shown in Figs. 7 and 8. In Fig. 7 we have represented the dependence of the temperature *vs*. time in the point situated on the top skin surface, at the center of the laser spot, for the geometries shown in Fig. 6 (without vessel, and with one, two and three pairs of vessels respectively). As expected, the cooling effect of the blood flow is more pronounced when the vessels are situated closely to the top surface of the skin and the flow rate is larger. On the other hand, as is shown in Fig. 8, the spatial distribution of the blood vessels has a very important influence on the thermal field in the skin. An appropriate blood vessel network can have a confinement effect on the temperature distribution Figs. 8a–d and this could be taken into consideration in real laser therapy procedures when a melanoma, for example, is situated close to a blood vessel network. Moreover, one can imagine different schemes for the dependence of the laser exposure function ($F(t)$ in eq. (2)) such that the temperature be maintained between specified values in a region of interest into the vascularized skin.

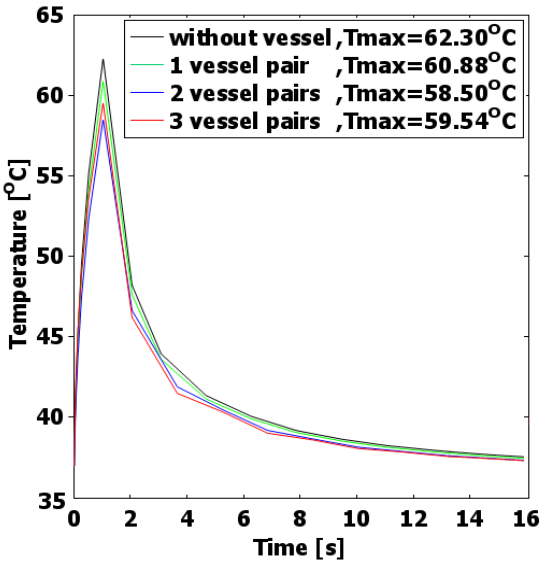

Fig. 7 – Dependence of the temperature *vs.* time in the point (x = 0.02 m; y = 0.02 m; z = 0.01 m).

The effect of the convective heat transfer is clearly shown in Figs. 8e–h where we have represented the temperature distribution $T(x, y)$ on the top skin

surface at the time t = 16 s. In the case of a skin block without blood vessel network the temperature distribution on the top skin surface is perfectly radial, the highest value of the temperature being attained in the middle of the Gaussian laser spot (Fig. 8e). On the other hand, the temperature distribution on the top skin surface has no more a circular symmetry but is elongated in the direction of the blood flow when a pair of artery-vein counter-current vessels is buried into the skin (Figs. 8f–h). We see also that the cooling effect of the blood flow is more important for smaller depth of the blood vessels.

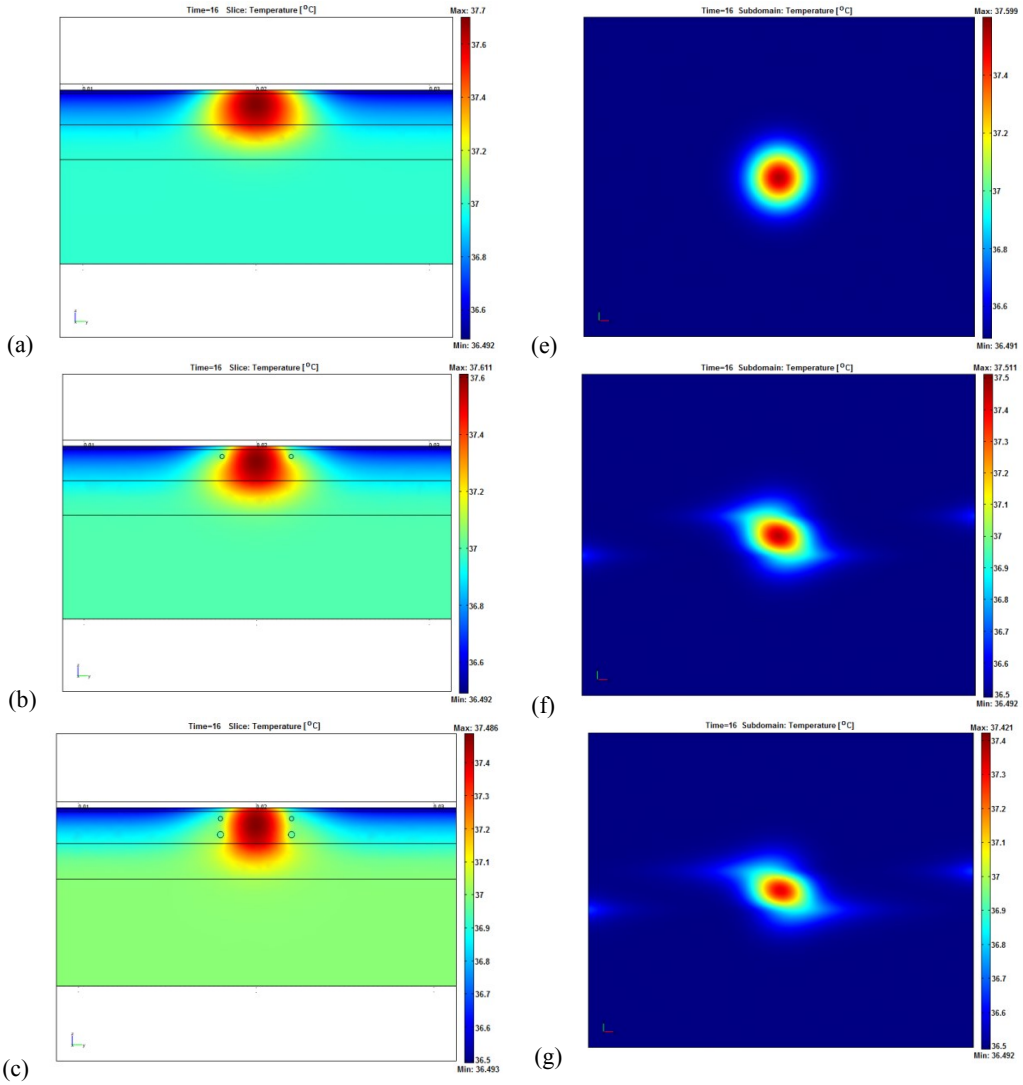

Fig. 8

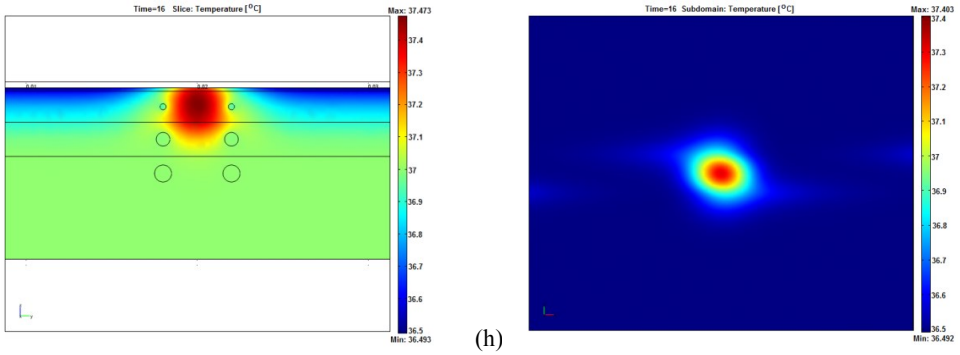

Fig. 8 (continued) – Temperature distribution in the middle *y*-*z* plane (a–d) and on the *x*-*y* skin surface (e–h) for a skin without vessels and with one, two, or three pairs of blood vessels respectively.

4. CONCLUSIONS

We have performed a numerical study regarding the cooling effect of blood flow during laser therapy of vascularized tissues. The model described in this study is very adaptable and easy to use on a variety of tissues, geometries, and laser exposer parameters. Our model uses the semi-infinite body approximation and a Gaussian incident laser beam. In our studies we supposed that the radiation is provided by a CO_2 laser. This radiation is highly absorbed by tissues and, moreover, its scattering in the irradiated medium could be neglected. In this case the model may be simplified because the Beer-Lambert's law may be used to calculate the photon distribution in tissue and the volumetric heat source is confined to a very thin region at the tissue surface. Once the concept of "surface heat source" is recognized to be valid in our case, the thermal field in the vascularized tissue was calculated by performing transient simulations using the finite element method. We have taken into consideration conductive and convective heat transfer in the vascularized tissue and convective heat transfer at the tissue-air interface. The parametric study on a homogeneous tissue containing a single buried blood vessel shows that the presence of the vessel, its depth relative to the top surface of the tissue, and the flow parameters (vessel radius and maximum velocity of the flow) clearly influence the temperature distribution in the irradiated vascularized tissue. These observations were confirmed by a supplementary study on a layered skin model containing different blood vessels networks.

A further step is this study will be to incorporate in the model the scattering of photons in tissue. This will be done by calculating the photon distribution into irradiated tissue by using the transport theory.

REFERENCES

1. L. Cummins, M. Nauenberg, Biophys. Journal **42**, 99-102 (1983).
2. J-L. Boulnois, Lasers in Medical Science **1**, 47-66 (1986).
3. T.J. Dougherty, C.J. Gomer, B.W. Henderson, G. Jori, D. Kessel, M. Korbelik, J. Moan, Q. Peng, Journal of the National Cancer Institute **90**, *12*, 889-905 (1998).
4. A.L. McKenzie, Physics in Medicine and Biology **35**, *9*, 1175-1209 (1990).
5. A.J. Welch, M. J. C. van Gemert (Eds.), *Optical-thermal Response of laser-irradiated Tissue*, Plenum Publishing Corporation, New York, 1995.
6. M.H. Niemz, *Laser-Tissue Interactions. Fundamentals and Applications,* 3rd Revised Edition, Springer-Verlag, Berlin Heidelberg, 2007.
7. Li Dong, He Ya Ling, Wang Guo Xiang, Wang Yong Xian, Ying Zhao Xia, Chinese Science Bulletin **58**, 416-426 (2013).
8. A.A. Meesters, L.H.U. Pitassi, V. Campos, A. Wolkerstorfer, C.C. Dierickx, Lasers in Medical Science **29**, 481-492 (2014).
9. D. Li, B. Chen, W.J. Wu, G.X. Wang, Y.L. He, Z.X. Ying, Lasers in Medical Science **30**, 135-145 (2015).
10. A. Vogel, V. Venugopalan, Chemical Reviews **103**, 577-644 (2003).
11. A. Welch, IEEE J. Quantum Electronics **20**, *12*, 1471-1481 (1984).
12. A. Paul, A. Narasimhan, F.J. Kahlen, S.K. Das, Journal of Thermal Biology **41**, 77-87 (2014).
13. M. Motamedi, A. Gonzales, A.J. Welch, *Thermal response of gastrointestinal tissue to Nd:YAG laser irradiation: A theoretical and experimental investigation*, Laser Inst. Amer., Los Angeles, CA, 1983.
14. J.C. Chato, J. Biomech. Engineering **102**, 110-118 (1980).
15. J.J.W. Lagendijk, Phys. Med. Biol. **27**, 17-23 (1982).
16. C.K. Charny, R.L. Levin, J. Biomech. Engineering **111**, 263-270 (1989).
17. Z.P. Chen, R.B. Roemer, J. Biomech. Engineering **114**, 473-481 (1992).
18. M.C. Kolios, M.D. Sherar, J.W. Hunt, Phys. Med. Biol **40**, 477 (1995).
19. J. Zhou, L. Liu, Numer. Heat Transfer. Part A: Appl. **45**, 415-449 (2004).
20. T.C. Shih, H.L. Liu, A.T.L. Horng, Int. Commun. Heat Mass Transfer **33**, 135-141 (2006).
21. Y. Mohammed, J.F. Verhey, BioMedical Engineering OnLine **4**, *2* (2005), doi:10.1186/ 1475-925X-4-2.
22. A. Bhowmik, R. Repaka, S.C. Mishra, Computers in Biology and Medicine **53**, 206-219 (2014).
23. H. Pennes, J. Applied Physics **1**, 93-122 (1948).
24. Y.A. Cengel, *Heat Transfer: A Practical Approach*, 2nd Edition, McGraw-Hill, Boston, 2002.
25. F.M. White, Fluid Mechanics, Fourth Edition, McGraw-Hill, Boston, 1998.
26. COMSOL AB, Stockholm (2008); www.comsol.se
27. A. Sagi, A. Shitzer, A. Katzir, S. Akselrod, Optical Engineering **31**, *7*, 1417-1424 (1992).